Progress In Electromagnetics Research C, Vol. 127, 157–169, 2022

C-Band Rectangular DRA with Defective Ground Structure for Satellite Uplink Applications

Syamala Misala* **and Satya Anuradha Mosa**

Abstract—The C-band RDRA with a defective ground structure operated at resonant frequency 6.2 GHz is best suitable for satellite uplink applications. In the C-band, the broad aperture slot and pentagonal-shaped defective ground structure (DGS) offer excellent isolation and great efficiency. The simple prototype of designed pentagonal DGS RDRA is fabricated, tested, and validated. The proposed C-band RDRA has a fractional bandwidth of 12.14%, a return loss of −30 dB, a gain up to 7.95 dB, and a minimal VSWR at the resonance frequency of 6.2 GHz. It offers a broad beamwidth of 110.87° in the E-plane, 43.73° in the H-plane, and 91.5% efficiency.

1. INTRODUCTION

A revolutionary high-speed wireless communication system in the new technology demands small, highly effective antennas. A wireless communication system would benefit from a rectangle dielectric resonator antenna (RDRA) because of its small size, light weight, and high efficiency [1]. With its circular slots, the low-profile, compact DRA [2] operates in a triple band with peak gains of 5.32 dB, 4.16 dB, and 4.87 dB and impedance bandwidths of 8.16%, 8.57%, and 6.1%. The circularly polarized dual-band RDRA with a triangular Aperture Couple was proposed by Gupta and Gangwar [3]. The impedance bandwidths of a unique circularly polarized dual-band DRA [4] are 17.0% (20.5 GHz–24.3 GHz) and 15.2% (26.1 GHz–30.4 GHz), with peak gains of 5 dB and 8 dB, respectively. The two-segment ring dielectric resonator [5] has a gain of 5.207 dB and an impedance bandwidth of 103.9%. It operates in the frequency range of 3.45 GHz to 10.9 GHz. Four alternative radiating frequencies are offered by the transformer-type microstrip feed RDRA [6] at 3.8, 6.4, 8.8, and 10 GHz. The peak gain is 7.2 dB, and it permits broaden impedance bandwidth (IMBW) 104.09% (3.28–10.4) GHz. With fractional bandwidths of 18.31% and 23.14%, the dual-polarized hybrid aperture DRA [7] with inverted pentagonal shape aperture operates in two frequency ranges (2.48 GHz–2.98 GHz) and (4.66 GHz–5.88 GHz) and is suitable for (2.5/5.5) WiMAX GHz and WLAN) applications. Circularly polarized dual band DRA [8] is suitable for downlink defense satellite applications as it operates in the frequency ranges (5.01 GHz–6.41 GHz) and (7.3 GHz–7.9 GHz) with IMBWs of 24.73% and 9.39%, respectively. A circular polarization dual-band microstrip antenna [9] has an efficiency of 92% and defective ground structure (DGS) in the lower and higher bands of 2.30 GHz to 2.48 GHz and 3.80 GHz to 3.9 GHz, respectively. The IMBWs are 7.5% and 2.94%. With a maximal gain of 7.68 dB, an "OM"-shaped elliptically polarized DRA [10] is used for WLAN, WIMAX, INSAT, and satellite X band RADAR applications. DRA [11] has circular polarization and a sizable impedance bandwidth of 62.07% (2.2 GHz–4.18 GHz). For AMSAT, GPS, point-to-point microwave, WLAN, WIMAX, and telemetry, a triple band hybrid RDRA [12] is excited with a composite feeding structure with IMBWs being 11.69%, 12.44%, and 25.19%, and gains are 1.6 dB, 2.34 dB, and 4.79 dB. A circularly polarized DRA [13] acquires 5.96 dB and 6.2 dB appropriate for wireless applications while operating in dual bands (lower & upper band) with IMBWs of 14.65% and 19.86%. Dual-band slot

Received 4 October 2022, Accepted 1 December 2022, Scheduled 11 December 2022
* Corresponding author: Syamala Misala (msyamala869@gmail.com).
The authors are with the Department of ECE, Andhra University, College of engineering, Visakhapatnam, Andhra Pradesh, India.

linked circular polarization [14] RDRA's gains are 5.4 dB and 5.8 dB, and IMBWs of the RDRA are 9.1% (1.58 GHz–1.73 GHz) and 14.4% (2.39 GHz–2.76 GHz). In order to create orthogonal modes in RDRA appropriate for 3G/WIMAX applications, the hybrid RDRA [15] is operated in four frequency bands: 1.81 GHz–2.06 GHz, 2.37 GHz–2.7 GHz, 3.35 GHz–4.4 GHz, and 4.62 GHz–5.62 GHz. With fractional bandwidths of 30.17% and 22.14% and peak gains of 2.45 dB and 3.89 dB, a ring DRA with a moon-shaped faulty ground structure [16] excites TE modes. A Zig-Zag shaped slit microstrip antenna with a defective ground structure covers frequency 2.45–5.28 GHz with a steady gain of 4 to 6 dB used for WLAN and WIMAX applications [17]. With a gain of 3.86 dB, a circularly polarized DRA [18] is reported with an impedance bandwidth of 26.84% from 2.94 to 3.85 GHz. A wideband circularly polarized RDRA [19] stimulated has a novel microstrip circular ring impedance bandwidth of 20.79% and gain of 5.07 dB connected through orthogonal slots. The RDRA is activated with an F-shaped slot [20] and has an impedance bandwidth of 50.55 percent, an average gain of 3.87 dB, and a radiation efficiency of 92%. Circular polarization properties are present in DRA stimulated with a square slot [21]. A cross aperture coupled spiral microstrip line feeding a circularly polarized RDRA [22] is suited for WIMAX applications. A circularly polarized RDRA [23] is fed by an elliptical slot aperture with an impedance bandwidth of 21.85% (5.34 GHz–6 GHz) GHz and gain of 5.9 dB with a 95% efficiency. A millimeter-wave RDRA [24] using a higher-order mode provides a measured 10-dB impedance bandwidth of 5.39%. The DRA's measured antenna gain at 24 GHz is 5.8 dBi. A slot-coupled millimeter-wave DRA [25] has a maximum gain of 6 dB and a bandwidth of 6.1% (58.8–62.5 GHz). An impedance bandwidth of 95.5% is presented by a low profile DRA [26] with dual-band circular polarization (CP) and wide impedance bandwidths from 3.66 GHz to 10.35 GHz, with an impedance bandwidth of 54.3%, a 3 dB axial ratio (4.31 GHz–7.53 GHz), a peak realized gain of 5 dB, and a radiation efficiency of 97%. A dual band circularly polarized compact equilateral triangular dielectric resonator antenna (TDRA) [27] has gains 2.15 dB and 69 dB in the frequency range (7.32–7.68) GHz and (8.34–9.44) GHz. Four open-ended logarithmic spiral slots are used to excite an omnidirectional circularly polarized DRA [28]; the resulting impedance bandwidth and 3-dB axial ratio (AR) bandwidth are 8.6% (2.33–2.54) GHz and 6.2%, respectively (2.35 GHz–2.50 GHz). A wideband trapezoidal DRA [29] is circularly polarized resulting in impedance bandwidth 33.5% (2.88–4.04) GHz, and 3-dB AR bandwidth 21.5% (3.11 GHz–3.86 GHz) with gain ranging from 5.28 dB to 8.40 dB. The two degenerate modes, TE111 and TE113, are concurrently excited by a circularly polarized slot coupled dual-band RDRA [30], whose impedance bandwidths are 9.1% and 14.4%, respectively. The impedance bandwidths of a dual-band, circularly polarized hybrid DRA [31] are 14.0% (1.80 GHz–2.07 GHz) and 12.8% (2.57 GHz–2.92 GHz), while the 3-dB AR bandwidths are 3.0% (1.97 GHz–2.03 GHz), 3.5% (2.79 GHz–2.89 GHz).

Square spiral strip feed [32] with an impedance bandwidth of 11% is used to excite RDRA (4 GHz–4.4 GHz). A 5 dB gain, 20% impedance bandwidth, and single feed excitation are used in a broad-band circular polarization RDRA [33]. For wireless body area network (WBAN) applications, an H-shaped conformal metal strip RDRA [34] with an impedance bandwidth of 20.7% (6.95 GHz–8.68 GHz) and gain of 5 dB is used. WLAN applications can benefit from the omnidirectional circularly polarized DRA [35] with Alford loop top loading, impedance bandwidth 10.8% (2.37 GHz–2.64 GHz), gain 1.12 dB, and efficiency 76%. A cylindrical, circularly polarized, slot-coupled DRA [36] has the gain of 4 dB and impedance bandwidth of 23% (4.5–5.6 GHz). The inverted-sigmoid circular polarization DR [37] operates in 5.51 GHz–7.46 GHz and 11.8 GHz–12.37 GHz frequency ranges, with gains of 4.85 dB and 6.38 dB, respectively, with an efficiency of 80%. A fan-shaped DRA with a rectangular slot [38] has gains of 3 dB and 4.2 dB and impedance bandwidths of 38.17% (2.84 GHz–4.18 GHz) and 33.75% (6.28 GHz–8.83 GHz). Suitable for satellite applications, a bowtie-shaped circularly polarized DRA [39] stimulated by microstrip line feed through a cross-shaped slot has an impedance bandwidth of 43.8% (6.75 GHz–10.53 GHz) and a gain of 5.8 dB.

Aperture linked feed, one of many fascinating feeding techniques, is applied in the current suggested work to reduce spurious radiations. For C-band satellite uplink applications, the suggested C-band RDRA with a flawed ground structure operating at resonant frequency 6.2 GHz offers a high impedance bandwidth and high efficiency. In the present paper, a single RDRA (Al_2O_3) having $\epsilon_{dr} = 9.8$ with U-shaped microstrip feed achieves impedance bandwidth 12.24% and high efficiency 90%. There are five sections in the paper. The introduction is in Section 1. The design and configuration of the antenna are covered in Section 2. The antenna design calculation is shown in Section 3. The simulated and

measured results of the proposed antenna are discussed in Section 4, and the conclusion is provided in Section 5.

2. DESIGN AND CONFIGURATION OF ANTENNA

Alumina Al_2O_3 (high-permittivity $\epsilon_r = 9.8$ and loss tangent 0.002) material is used to create the suggested C-band rectangle DR. High return loss and impedance bandwidth are made possible by the DGS idea employed in RDRA. The fabrication is easy with Alumina because of its availability. The substrate and ground are of the same size $S_x \times S_y$, i.e., the length (S_x) and breadth (S_y) are 46 mm. The selected substrate is made of glass epoxy FR4, with its relative permittivity $\epsilon_r = 4.4$, loss tangent = 0.02, and thickness $S_t = 1.5$ mm. The wide aperture slot is coupled with a designed microstrip line of feed length $f_L = 29$ mm and feed width $f_w = 2$ mm. The stripline has a 4 mm length and a U-shaped aperture at one end. The energy fields are connected into the RDRA through a large aperture slot that has the dimensions length = 18 mm and width $S_W = 9.5$ mm. By using parametric analysis, the proposed RDRA's height $H_t = 15$ mm and width $2R = 14$ mm are improved. The side length L and pentagonal DGS thickness are 2.1 mm and 0.5 mm, respectively. Figure 1 shows the suggested antenna's construction view using Al_2O_3 Alumina. The proposed antenna's geometry parameters are shown in Table 1.

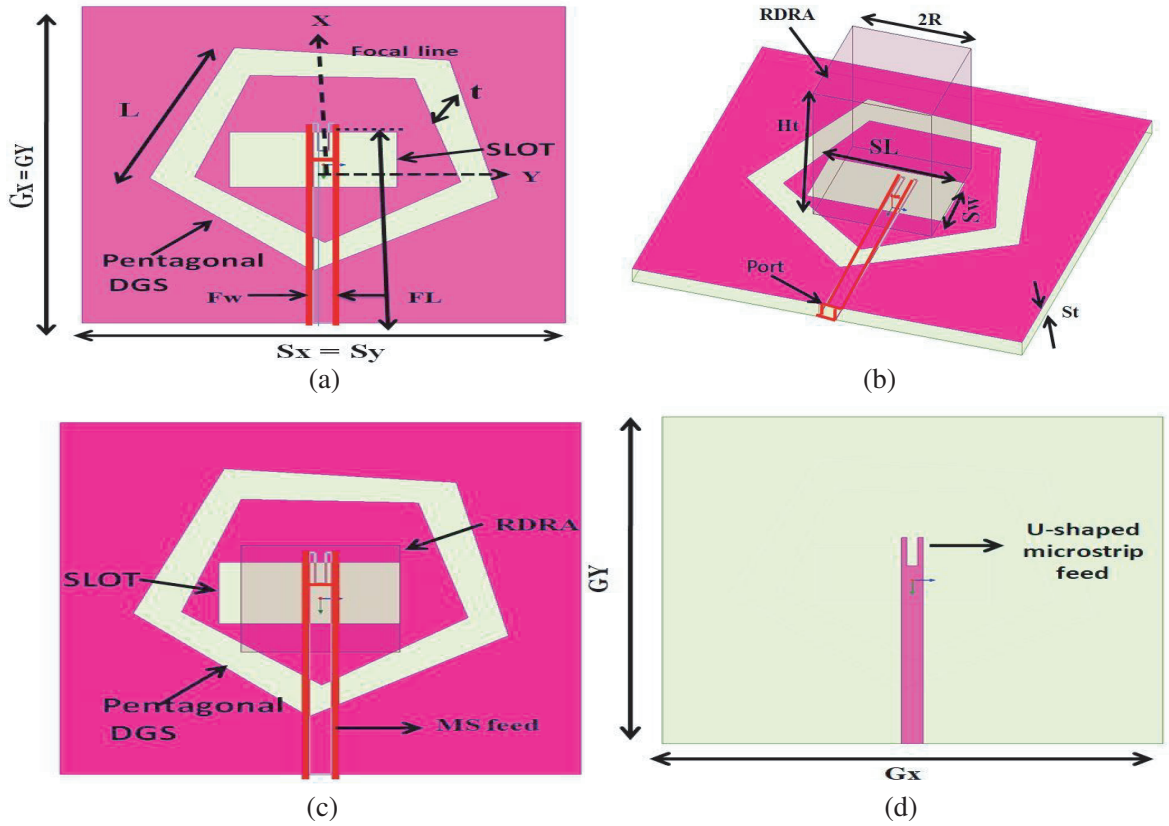

Figure 1. The construction view of antenna. (a) Top view with wide pentagonal-shaped DGS without RDRA. (b) Trimetric view with RDRA. (c) Top view with RDRA. (d) Bottom with U-shaped microstrip feed.

The E-field distribution of the ground-plane pentagon-shaped defective ground structure (DGS) in the wide aperture is shown in Figure 2. In the E-field distribution, the colour Red denotes the high concentration, and the colour Blue denotes the low concentration in the scale for rectangular DRA at 6.2 GHz resonance. There is a 90° step phase difference among Figures 2(a), (b), (c), and (d). Both

Table 1. Parameters of proposed antenna pentagonal DGS with RDRA.

S. No.	Name of the Parameter	Parameter	Value (mm)
1	RDRA height	H_t	15
2	RDRA Width/length	$2R$	14
3	Substrate thickness	S_t	1.6
4	Slot width	S_W	9.5
5	Slot Length	S_L	18
6	Substrate Length	$S_x = S_y$	46
7	Ground plane length	$G_x = G_y$	46
8	Microstrip feed Length	F_L	29
9	Microstrip feed width	F_W	2
10	The thickness of pentagonal DGS	t	0.5
11	Side of the length of the pentagonal (L)	L	2.1

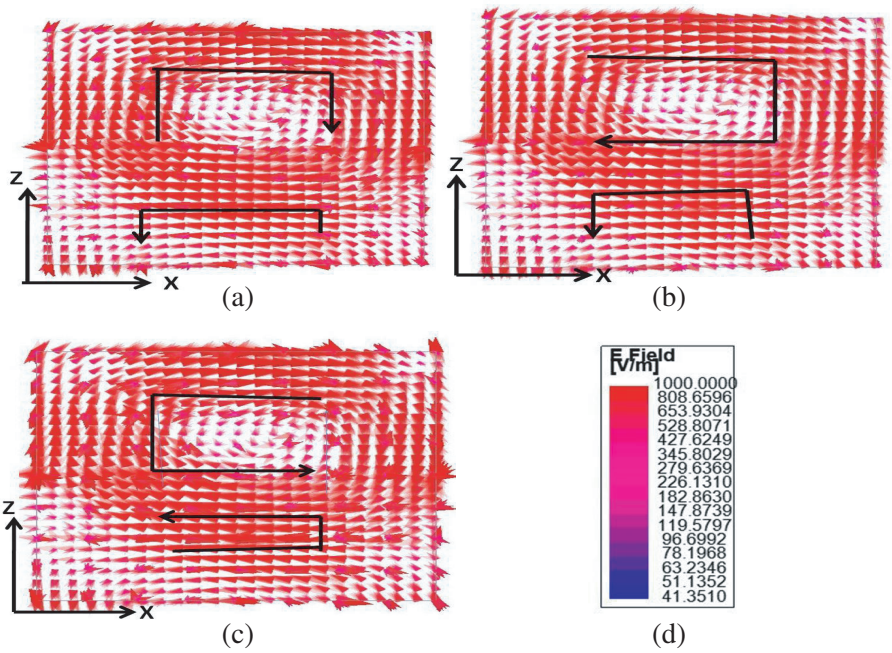

Figure 2. E field distribution of antenna in right side view. (a) Phi = 0°. (b) Phi = 90°. (c) Phi = 180°. (d) Scale for (a), (b), (c) and at 6.2 GHz.

clockwise and counterclockwise motions are present in the E-fields. Figures 3(a), (b), (c), and (d) show surface current distributions of isometric view and top view with DRA. The current is moving in the ground plane and pentagonal DGS edges. The current mainly focuses on the U-shaped microstrip feed line, and it is observed within the DRA. It is noticed that the electric field and surface current movements are uniform. Figure 4 shows the three-dimensional radiation far-field pattern of the proposed C-band antenna simulated by Ansoft HFSS at 6.2 GHz. Electric field and surface current motions are shown to be uniform. The suggested C-band antenna's three-dimensional radiation far-field pattern is depicted in Figure 4 and was generated by Ansoft HFSS at 6.2 GHz. The ground defected when slot is created in it, it disturbs the current distribution, and it changes the characteristics of a transmission line. Thus, the line impedance is changed.

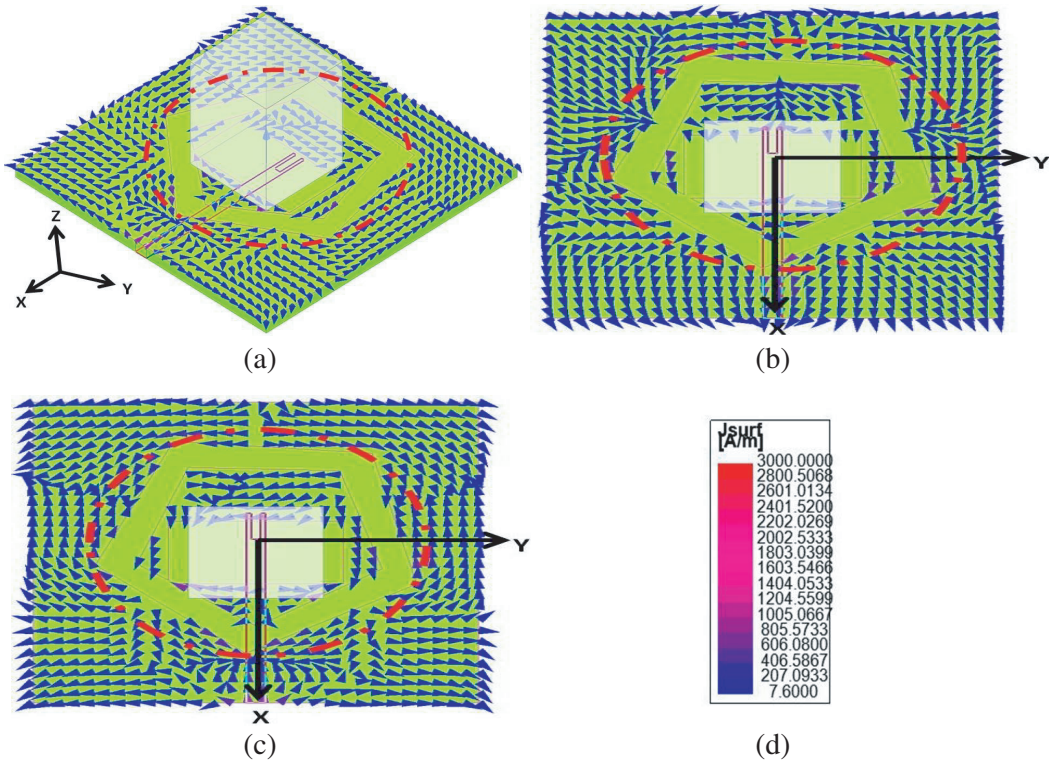

Figure 3. Surface current movement of antenna. (a) Isometric view (XYZ) Phi = 0°. (b) Top view (XY) Phi = 90°. (c) Top view (XY) Phi = 180°. (d) Scale for (a), (b), & (c) at 6.2 GHz.

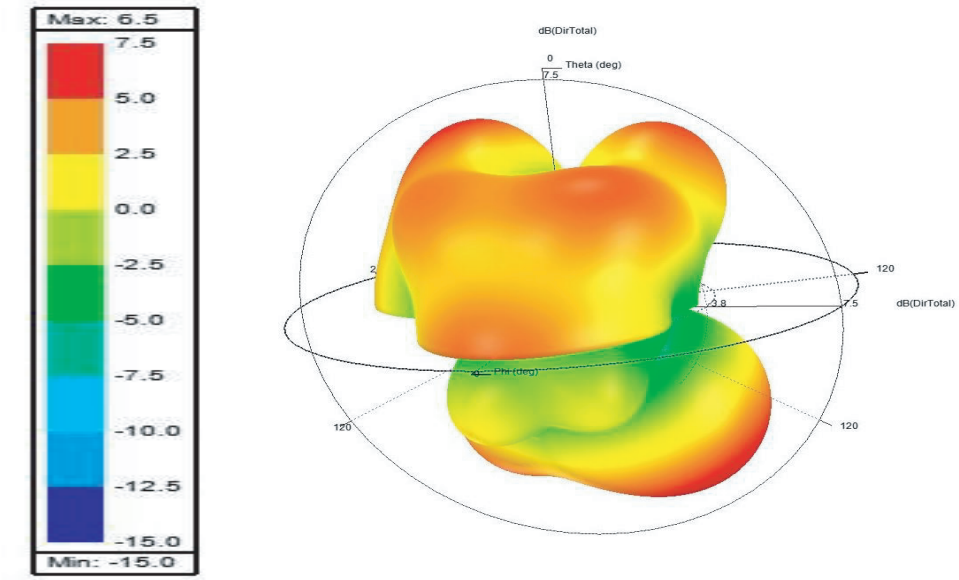

Figure 4. 3D radiation far-field pattern of the proposed antenna.

3. ANTENNA DESIGN CALCULATION

The C-band rectangle DRA with pentagonal DGS substrate is made of FR4 glass epoxy, and the ground has the same length (S_x) and breadth (S_y) of 46 mm, as shown in Figure 1. The resonant frequency

of RDRA depends on the dielectric material's dielectric constant. The rectangular dielectric resonator antenna (RDRA) resonant frequency is calculated by the following Equation,

$$f_{res} = \frac{397}{2\pi R}(C_0 R) \tag{1}$$

$$where\ R = 1/2\ width\ of\ RDRA$$

$$C_0 R = \frac{1.6 + 0.513k + 1.392k^2 - 0.575k^3 + 0.088k^4}{\epsilon_{d_R}^{0.42}} \tag{2}$$

$$k = \frac{R}{2 * H_t}$$

The substrate dielectric constant $\epsilon_{dR} = 9.8$, $H_t = 15\,\text{mm}$ & $R = 7\,\text{mm}$. Then resonant frequency $f_{res} = 6.2\,\text{GHz}$.

4. ANTENNA ANALYSIS

The C band rectangular dielectric resonator antenna (RDRA) has a large aperture slot and a ground plane with a pentagonal-shaped DGS. Since the aperture slot serves as a magnetic current element and accelerates the magnetic field into DRA, it prevents spurious radiations. The parametric analysis at resonance frequency 6.2 GHz reveals that the return loss is considerable at RDRA height = 15 mm. Figures show the suggested antenna near E-field distributions, surface current distributions, and 3D far field pattern discovered at a resonant frequency of 6.2 GHz (2–4). Pentagon-shaped DGS and aperture slots exhibit consistent electric field and surface current motions. Figure 5 depicts the proposed antenna after fabrication (a) Pentagonal DGS with top view of RDRA, (b) DGS RDRA 3D view of the pentagon, (c) With SMA connector, the back view. To verify the results of the simulation, the proposed antenna was manufactured and measured. Figure 6(a) displays the measurement setup using an Anritsu vector network analyzer with model number VNA MS2037C for reflection coefficient and VSWR (b). A typical waveguide horn antenna (1 GHz–40 GHz) is used to assess the proposed antenna's gain and efficiency in an anechoic chamber using the key sight signal generator N5173 B, as shown in Figure 7(a) & (b). The parameters of the proposed simulated and measured results are given to the antenna in Table 3, and Table 2 compares the impedance bandwidth simulated and measured results.

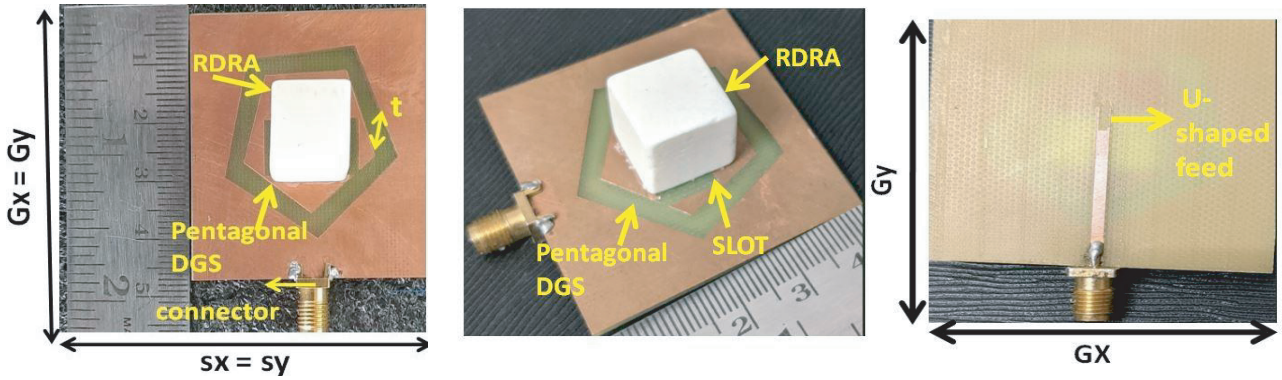

(a) (b) (c)

Figure 5. (a) Top view fabricated antenna. (b) Antenna 3D view. (c) Antenna back side view.

The proposed fabricated antenna structure operated in a single frequency band, i.e., 5.75 GHz–6.5 GHz, with a fractional bandwidth of 12.24% at the center frequency. There is some difference between the simulated and measured results due to the effect of SMA (50 Ω) and adhesive connector.

Table 2. Comparison of impedance bandwidth of proposed antenna simulated with measured result.

Simulated & Measured	Resonant frequency (GHz)	Frequency Range (GHz)	Fractional Bandwidth
HFSS	6.2	5.8–6.55	12.14%
Measured	6.125	5.75–6.5	12.24%

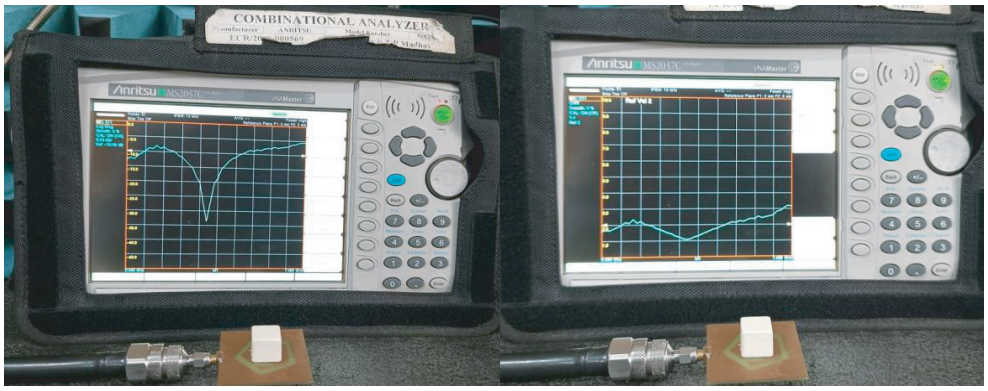

(a) (b)

Figure 6. Pentagonal shaped DGS with RDRA. (a) Measurement setup for reflection coefficient. (b) Measurement setup for VSWR.

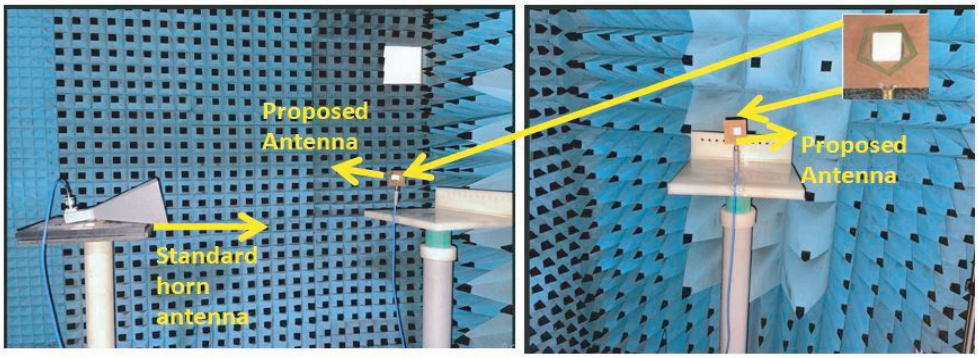

(a) (b)

Figure 7. Measurement setup for (a) gain and (b) RDRA with pentagonal DGS.

Table 3. Comparison of simulated and measured antenna parameters of proposed design.

S. No.	Antenna Parameters	Simulated	Measured
1	Return Loss (dB)	30	33
2	VSWR (abs)	01	1.1
3	E-plane co-polarization 3 dB beam width (dB) E-plane cross-polarization 3 dB beam width (dB)	110.87° 67.82°	114.92° 68.84°
4	H-plane co-polarization 3 dB beam width (dB) H-plane cross-polarization 3 dB beam width (dB)	43.73° 44.66°	42.76° 43.56°
5	Peak Gain (dB)	4.95–7.95	3.95–7.75
6	Radiation Efficiency (%)	91.5%	90%

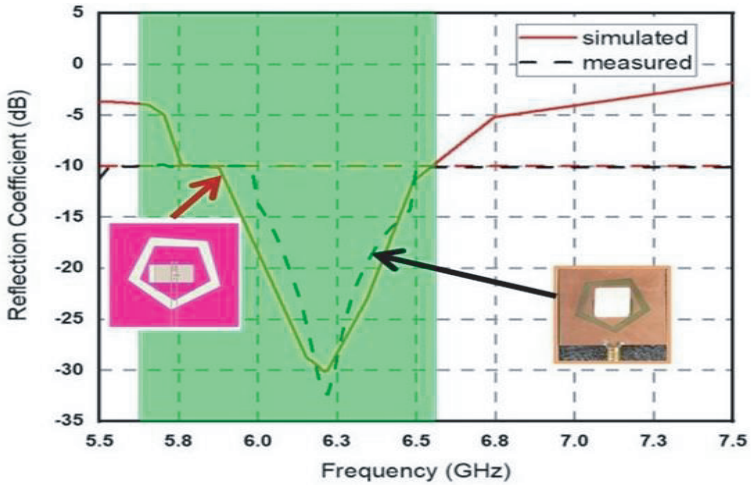

Figure 8. Reflection coefficient versus frequency.

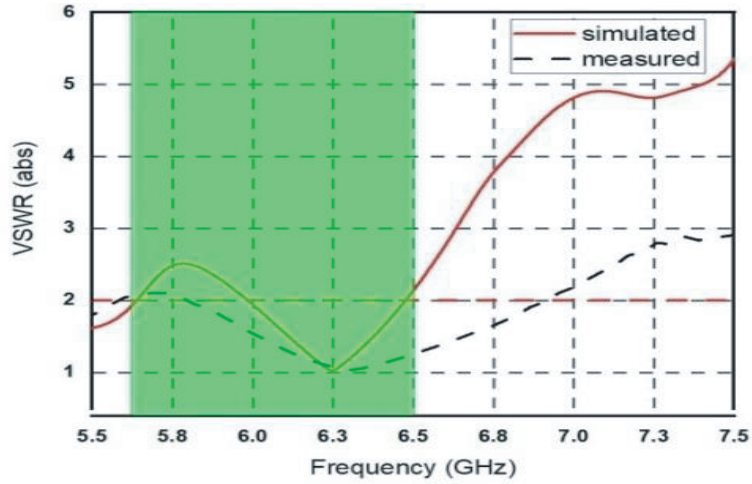

Figure 9. VSWR versus frequency.

Table 4. The comparisons of the proposed RDRA with pentagonal DGS with previous researcher works.

Ref. No.	Type of Antenna	f_r (GHz)	FBW (%)	Gain (dB)	Efficiency (%)
18	RDRA	3.4	26.84%	3.86	87%
19	RDRA	3.27	20.79%	5.07	84%
21	RDRA	5.5	9.25%	4.75	95%
23	RDRA	5.85	21.85%	5.9	95%
30	RDRA	1.65 2.57	9.1% 14.4%	5.4 5.8	NA
31	RDRA	2.84	14.0% 12.8%	5.65	NA
PW	RDRA	6.2	12.24%	7.95	90%

5. RESULTS

The C band RDRA with pentagonal DGS resonates at 6.2 GHz, which is suitable for satellite uplink applications. It can be used to track weather RADAR & rugged wireless communications. The pentagonal DGS technique with a designed U-shape microstrip feed is employed in this paper and improves gain and high efficiency. Simulated and measured results of pentagonal DGS with RDRA parameters are presented in Figure 8–Figure 13. It is observed that measured and simulated results are identical. From Table 2, the proposed C-band RDRA with pentagonal DGS is simulated with

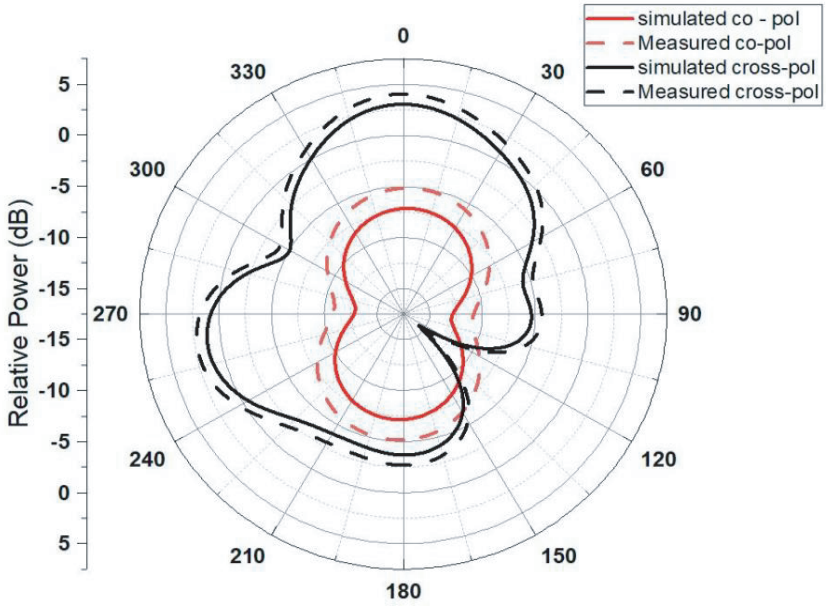

Figure 10. 2D radiation pattern E-plane.

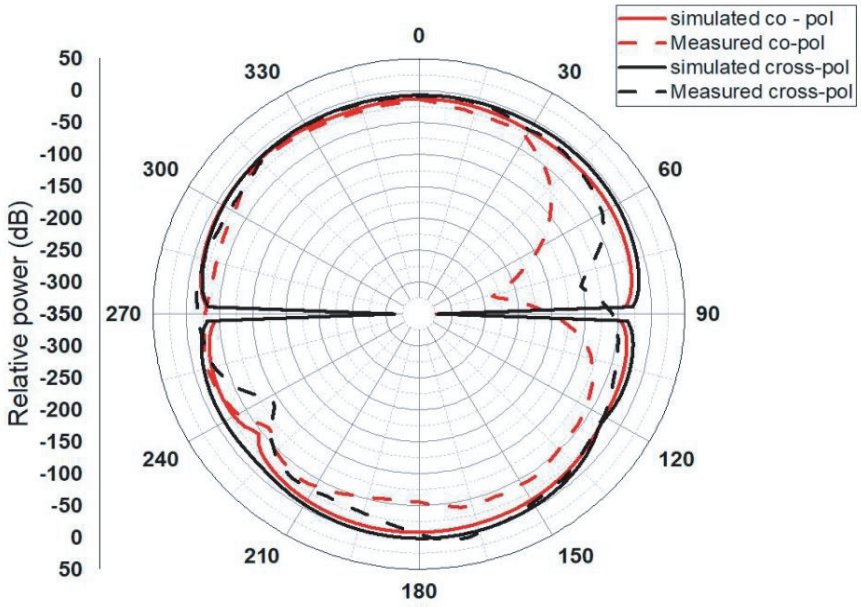

Figure 11. 2D radiation pattern H-plane.

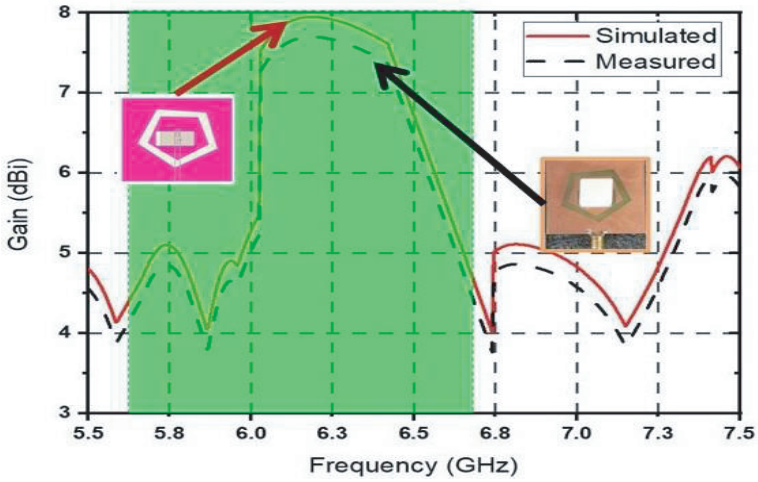

Figure 12. Gain versus frequency.

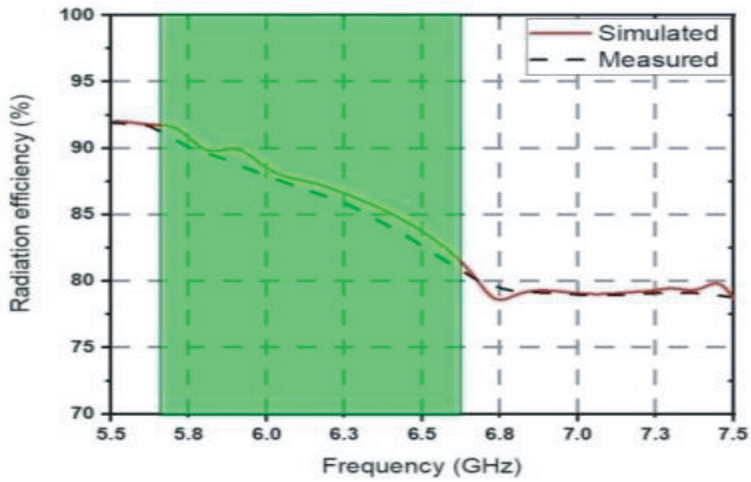

Figure 13. Radiation efficiency versus frequency.

a fractional bandwidth (FBW) of 12.14% (5.8 GHz–6.55 GHz) and measured with FBW of 12.24% (5.75 GHz–6.5 GHz), shown in Figure 8. The simulated and measured voltage standing wave ratios are 1 and 1.1 in Figure 9. Figure 10 shows the E-plane 3 dB co-polarization beamwidth simulated 110.87° and measured 114.92°, and 3 dB cross-polarization beamwidth simulated 67.82° and measured 68.84°. Figure 11 shows that the 2D far-field pattern is omnidirectional. Its simulated H-plane 3 dB co-polarization beamwidth is 43.73°, and measured one is 42.76°. Its simulated 3 dB cross-polarization beamwidth is 44.66°, and measured one is 43.56°. Figure 12 shows that the proposed antenna simulated gain is 4.95 dB–7.95 dB in the frequency band (5.8 GHz–6.55 GHz), and the measured gain is 4.0 dB–7.75 dB in the frequency band (5.75 GHz–6.5 GHz). There is a minor difference between the gain values due to the connector losses and cable losses in the measurement and simulated. Figure 13 shows that simulated and measured radiation efficiencies are 91.5% and 90%. Half-power beamwidths are 114.92° and 42.76° at 6.2 GHz in E-plane and H-plane, respectively. The measured gain of the antenna is 4.0 dB–7.75 dB in the frequency band 5.8 GHz–6.55 GHz. The measured efficiency of the antenna is 90% in the frequency band 5.75–6.5 GHz. Table 4 compares the parameters of the designed and fabricated DRA with the designed DRAs in the literature.

ACKNOWLEDGMENT

The authors would like to thank the Antenna laboratory team, KL University, Guntur, Andhra Pradesh, India, for their assistance in the fabrication and measurement of the antenna prototype model.

REFERENCES

1. Petosa, A., A. Ittipibon, Y. M. MAntar, D. Roscoe, and M. Cuhaci, "Recent advances in dielectric-resonator antenna technology," *IEEE Antennas and Magazine*, Vol. 40, No. 3, June 1998.
2. Sharma, A. and R. K. Gangwar, "Compact triband cylindrical dielectric resonator antenna with circular slots for wireless application," *Journal of Electromagnetic Waves and Applications*, Vol. 30, No. 3, 331–340, 2016.
3. Gupta, A. and R. K. Gangwar, "Dual-band circularly polarized aperture coupled rectangular dielectric resonator antenna for wireless applications," *IEEE Access*, Vol. 6, 11388–11396, March 16, 2018.
4. Liu, Y., Y.-C. Jiao, and Z. Weng, "A novel millimeter-wave dual-band circularly polarized dielectric resonator antenna," *International Journal of RF and Microwave Computer-Aided Engineering*, Vol. 29, No. 10, 7 pages, May 25, 2019.
5. Sharma, A. and R. K. Gangwar, "Hybrid two segments ring dielectric resonator antenna for ultra wideband application," *International Journal of RF and Microwave Computer-Aided Engineering*, Vol. 26, No. 1, January 2016.
6. Yadav, S. K., M. Kaur, and R. Khanna, "Cylindrical air spaced high gain dielectric resonator antenna for ultra-wideband applications," *Sadhana*, Vol. 45, Article number: 163, Indian Academy of Sciences, June 26, 2020.
7. Sharma, A., G. Das, and R. K. Gangwar, "Dual-band dual-polarized hybrid aperture-cylindrical dielectric resonator antenna for wireless applications," *International Journal of RF and Microwave Computer-Aided Engineering*, Vol. 27, No. 5, e21092, January 20, 2017.
8. Gupta, S., A. Sharma, G. Das, and R. K. Gangwar, "A dual-band circularly polarized antenna with the aid of dual cylindrical dielectric resonator blocks," *International Journal of RF and Microwave Computer-Aided Engineering*, Vol. 29, No. 4, e21592, October 16, 2018.
9. Gautam, A. K. and B. K. Kanaujia, "A novel dual-band asymmetric slit with defected ground structure microstrip antenna for circular polarization operation," *Microwave and Optical Technology Letters*, Vol. 55, No. 6, 1198–1201, June 2013.
10. Yadav, S. K., A. Kaur, and R. Khanna, "An ultra-wideband "OM" shaped DRA with a defected ground structure and dual polarization properties for 4G/5G wireless communications," *International Journal of RF and Microwave Computer-Aided Engineering*, Vol. 30, No. 8, 18 pages, April 6, 2020.
11. Altaf, A. and M. Seo, "Dual-band circularly polarized dielectric resonator antenna for WLAN and WiMAX Applications," *Sensors*, Vol. 20, 1137, 2020.
12. Gupta, A. and R. K. Gangwar, "Hybrid rectangular dielectric resonator antenna for multiband applications," *IETE Technical Review*, February 06, 2019.
13. Kumari, R. and R. K. Gangwar, "Circularly polarized cylindrical dielectric resonator antenna excited by square ring slot with a T-shaped microstrip line," *Microwave and Optical Technology Letters*, Vol. 59, No. 10, 2507–2514, March 24, 2017.
14. Zou, M. and J. Pan, "A simple dual-band circularly polarized rectangular dielectric resonator antenna," *Progress In Electromagnetic Research Letter*s, Vol. 53, 57–63, 2015.
15. Sahu, K., A. Sharma, and R. K. Gangwar, "Dual-sense dual-polarized hybrid rectangular dielectric resonator antenna for multiband applications," *Progress In Electromagnetic Research C*, Vol. 74, 161–170, 2017.
16. Sharma, A. and R. K. Gangwar, "Compact dual-band ring dielectric resonator antenna with moon-shaped defected ground structure for WiMAX/WLAN applications," *International Journal of RF and Microwave*, Vol. 26, No. 6, 503–511, August 2016.

17. Sanjeeva Reddy, B. R. and D. Vakula, "Compact zig zag shaped slit microstrip antenna with circular defected ground structure for wireless applications," *IEEE Antennas and Wireless Propagation Letters*, Vol. 14, 678–681, 2014.
18. Kumar, R., S. R. Thummaluru, and R. K. Chaudhary, "Improvements in Wi-MAX reception, a new dual-mode wideband circularly polarized dielectric resonator antenna," *IEEE Antennas and Propagation Magazine*, Vol. 61, No. 1, 41–49, February 2019.
19. Kumar, R. and R. K. Chaudhary, "Circularly polarized rectangular DRA coupled through orthogonal slot excited with microstrip circular ring feeding structure for Wi-MAX applications," *International Journal of RF and Microwave Computer-Aided Engineering*, Vol. 28, No. 1, e21153, January 2018.
20. Kumar, R. and R. K. Chaudhary, "Investigation of higher order modes excitation through F-shaped slot in rectangular dielectric resonator antenna for wideband circular polarization with broadside radiation characteristics," *International Journal of RF and Microwave Computer-Aided Engineering*, Vol. 28, No. 6, e21281, August 2018.
21. Kumari, R. and R. K. Gangwar, "Circularly polarized slot coupled square dielectric resonator antenna for WLAN applications," *Microwave Optical Technology Lett.*, Vol. 60, No. 11, 2787–2794, 2018.
22. Kumari, R. and R. K. Gangwar, "Circularly polarized rectangular dielectric resonator antenna fed by a cross aperture coupled spiral microstrip line," *International Journal of RF and Microwave Computer-Aided Engineering*, Vol. 28, No. 2, e21200, February 2018.
23. Usha, L. and K. Kandasamy, "Circularly polarized rectangular dielectric resonator antenna with elliptical aperture feed for 5 GHz ISM band," *International Journal of RF and Microwave Computer-Aided Engineering*, Vol. 31, No. 12, 8 pages, 2021.
24. Pan, Y.-M. and K. W. Leung, "Design of the millimeter-wave rectangular dielectric resonator antenna using a higher-order mode," *IEEE Transactions on Antennas and Propagation*, Vol. 59, No. 8, 2780–2788, August 2011.
25. Ohlsson, L. and T. Bryllert, "Slot-coupled millimeter-wave dielectric resonator antenna for high-efficiency monolithic integration," *IEEE Transactions on Antennas and Propagation*, Vol. 61, No. 4, April 2013.
26. Meher, P. R., B. R. Behera, and S. K. Mishra, "Broadband circularly polarized cylindrical dielectric resonator antenna for wideband applications," *2019 TEQIP III Sponsored International Conference on Microwave Integrated Circuits, Photonics and Wireless Networks (IMICPW)*, 19256866, Tiruchirappalli, India, May 22–24, 2019.
27. Dash, S. K. K., T. Khan, and B. K. Kanaujia, "Circularly polarized dual facet spiral fed compact triangular dielectric resonator antenna for sensing applications," *IEEE Sensors Letters*, Vol. 2, No. 1, March 2018.
28. Yang, N., K. W. Leung, K. Lu, and N. Wu, "Omni directional circularly polarized dielectric resonator antenna with logarithmic spiral slots in the ground," *IEEE Transactions on Antennas and Propagation*, Vol. 65, No. 2, 839–844, 2016.
29. Pan, Y. and K. W. Leung, "Wideband circularly polarized trapezoidal dielectric resonator antenna," *IEEE Antennas and Wireless Propagation Letters*, Vol. 9, 588–591, 2010.
30. Zou, M. and J. Pan, "A simple dual-band circularly polarized rectangular dielectric resonator antenna," *Progress In Electromagnetic Research Letters*, Vol. 53, 57–63, 2015.
31. Zou, M., J. Pan, L. Zuo, and Z.-P. Nie, "Investigation of a cross-slot-coupled dual-band circularly polarized hybrid resonator antenna," *Progress In Electromagnetic Research C*, Vol. 53, 187–195, 2014.
32. Mohammad, S. and Salam K. Khamas, "A singly fed rectangular dielectric resonator antenna with a wideband circular polarization," *IEEE Antennas and Wireless Propagation Letters*, Vol. 9, 615–618, 2010.
33. Mohammad, S. and S. K. Khamas, "A singly fed wideband circularly polarized dielectric resonator antenna using concentric open half-loops" *IEEE Antennas and Wireless Propagation Letters*, Vol. 10, 2011.

34. Illahi, U., J. Iqbal, M. I. Sulaiman, M. M. Alam, et al., "Design of new circularly polarized wearable dielectric resonator antenna for off-body communication in WBAN applications," *IEEE Acces*, Vol. 7, 150573–150582, 2019.
35. Li, W. W. and K. W. Leung, "Omnidirectional circularly polarized dielectric resonator antenna with top-loaded Alford loop for pattern diversity design," *IEEE Transactions on Antennas and Propagation*, Vol. 61, No. 8, 4246–4256, August 2013.
36. Leung, K. W., W. C. Wong, and H. K. Ng, "Circularly polarized slot-coupled dielectric resonator antenna with a parasitic patch," *IEEE Antennas and Wireless Propagation Letters*, Vol. 1, 57–59, 2002.
37. Varshney, G., S. Gotra, V. S. Pandey, and R. S. Yaduvanshi, "Inverted-sigmoid shaped multi-band dielectric resonator antenna with dual band circular polarization," *IEEE Transactions on Antennas and Propagation*, Vol. 66, No. 4, 2067–2072, 2018.
38. Varshney, G., V. S. Pandey, and R. S. Yaduvanshi, "Dual-band fan-blade-shaped circularly polarized dielectric resonator antenna," *IET Microwaves, Antennas & Propagation*, 10.1049/iet-map.2017.0244.
39. Chauthaiwale, P., R. K. Chaudhary, and K. V. Srivastava, "Circularly polarized bowtie shaped dielectric resonator antenna excited with asymmetric cross slot," *Microwave and Optical Technology Letters*, Vol. 57, No. 7, 1723–1727, July 2015.